Analytical Methods

Indexed in Medline!

ROYAL SOCIETY OF CHEMISTRY

PAPER
Zachary D. Schultz *et al.*
Identification and quantification of pigments in plant leaves using thin layer chromatography-Raman spectroscopy (TLC-Raman)

PAPER

Check for updates

Identification and quantification of pigments in plant leaves using thin layer chromatography-Raman spectroscopy (TLC-Raman)†

Taylor D. Payne, [ID] [a] Lily R. Dixon,[a] Fiona C. Schmidt,[a] Joshua J. Blakeslee,[bc] Alison E. Bennett[d] and Zachary D. Schultz [ID] *[a]

Carotenoids are yellow, orange, and red pigments commonly found in plants. In leaves, these molecules are essential for photosynthesis, but they also play a major role in plant growth and development. Efficiently monitoring concentrations of specific carotenoids in plant tissues could help to explain plant responses to environmental stressors, infection and disease, fertilization, and other conditions. Previously, Raman methods have been used to demonstrate a correlation between plant fitness and the carotenoid content of leaves. Due to solvatochromatic effects and structural similarities within the carotenoid family, current Raman spectroscopy techniques struggle to assign signals to specific carotenoids with certainty, complicating the determination of amounts of individual carotenoids present in a sample. In this work, we use thin layer chromatography-Raman spectroscopy, or TLC-Raman, to identify and quantify carotenoids extracted from tomato leaves. These quick and accurate methods could be applied to study the relationship between pigment content and a number of factors affecting plant health.

Introduction

Carotenoids, a class of secondary photosynthetic pigments synthesized in plants, are vital to survival and extremely important for plant health. Not only are carotenoids essential for harvesting light in leaves, but they are also precursors of molecules responsible for plant signaling and growth regulation.[1,2] Additionally, carotenoids serve as photoprotectors and antioxidants and function to quench reactive oxygen species (ROS) generated during multiple plant stress responses. ROS produced in chloroplasts under stress can oxidize carotenoids to derivates which in turn are able to help the plant adjust to the stress conditions.[3–5] Additionally, carotenoid-mediated ROS quenching can prevent damage to the photosynthetic machinery co-localized in the chloroplast. Interestingly, genetic modification to the carotenoid biosynthesis pathway results in improved fitness, greater stress tolerance, and increased plant biomass.[6] Besides being crucial participants in complex plant metabolic pathways, carotenoids are also critical to human nutrition,[7] making them a relevant topic of study in many fields.

Raman spectroscopy is a powerful tool to rapidly and nondestructively elucidate the chemical composition of samples based on light scattering interactions. Recent studies have investigated the Raman signals arising from plant leaves under various conditions in efforts to develop noninvasive methods for diagnosing plant health. Many reports reveal carotenoids as candidate biomarkers for plant well-being. For instance, Raman leaf-clips and portable Raman systems have been used to monitor carotenoid content of leaves of plants experiencing nitrogen deficiency and other abiotic stressors, suggesting that a reduction in carotenoid signal is an indicator of plant stress.[8,9] Additionally, a decline in the Raman intensity of carotenoid peaks from leaves has been observed in correlation with viral and fungal infection in plants.[10,11] Plant exposure to metal toxicities has also been associated with decreased amounts of carotenoids by Raman imaging of leaves.[12] These studies highlight the potential for Raman spectroscopy to monitor carotenoid levels in leaves as a measure of plant health.

However, quantifying Raman signals from specific carotenoids, rather than bulk carotenoids, within plant leaves remains a challenge using spectroscopic signatures alone. The Raman spectra of carotenoids, which arise primarily from vibrations of the polyene chain, are highly sensitive to their environment. The polarity and polarizability of the solvent and other surrounding molecules can shift the position of the C=C Raman stretching bands of these molecules.[13] Additionally, many common plant carotenoids, such as β-carotene, lutein,

[a] Department of Chemistry and Biochemistry, The Ohio State University, Columbus, Ohio 43210, USA. E-mail: schultz.133@osu.edu

[b] Department of Horticulture and Crop Sciences, The Ohio State University, Columbus, Ohio 43210, USA

[c] Laboratory for the Analysis of Metabolites from Plants (LAMP) Metabolomics Facility, The Ohio State University, Columbus, Ohio, 43210, USA

[d] Department of Evolution, Ecology, and Organismal Biology, The Ohio State University, Columbus, Ohio 43210, USA

† Electronic supplementary information (ESI) available: Fig. S1–S6 with additional TLC plate images, Raman spectra of chlorophyll spots, standard addition curve, *etc.* (PDF). See DOI: https://doi.org/10.1039/d4ay00082j

zeaxanthin, lycopene, *etc.*, are very similar in structure and exhibit similar Raman spectra but with slight shifts in the Raman band frequencies based on the length of the polyene chain.[14] Moreover, carotenoids exhibit resonance Raman behavior when excited with light similar in energy to their absorbance profiles, and laser excitation wavelength has been shown to influence the position of the C=C stretch.[15] Together, these factors complicate both the identification and quantification of carotenoids in plant tissues by Raman spectroscopy.

Alternatively, liquid chromatography or liquid chromatography mass spectrometry methods (HPLC-DAD/PDA/UV-Vis/MS-MS) are often used to analyze carotenoid content of plant samples.[16–21] These procedures require lengthy sample preparation and run times, along with significant method development in some cases. Prior work investigating Raman signals of plant leaves has indicated challenges in statistically significant quantification of individual carotenoids using supplementary techniques such as HPLC.[22] Instead, we have developed a relatively simple and quick thin layer chromatography (TLC)-Raman method which allows for the separation, identification, and quantification of a specific carotenoid of interest. TLC is a powerful and inexpensive analytical tool for molecular identification based on comparison of retention factor (R_f) values to standards, and it conveniently allows Raman spectra to be obtained directly from the separated components on the plate. The Raman spectral fingerprint in combination with the R_f value of the molecule gives a more complete identity confirmation along with a quantifiable vibrational signal.

Raman signals from analytes on silica TLC plates have previously been reported, for instance from amino acids and small organic molecules.[23,24] More common are TLC-surface enhanced Raman spectroscopy (SERS) methods, which use metal nanostructures to increase Raman signals for detection of molecules at low concentrations. TLC-SERS has been employed to separate and quantify analytes in a variety of applications, such as reaction progress monitoring, food safety analysis, *etc.*[25–28] Quantitative TLC-Raman remains a relatively unexplored technique for plant pigment analysis.

In this work, we demonstrate TLC-Raman quantification of β-carotene, a carotenoid of particular interest, in tomato plant leaf extracts. Green leaves have been found to contain significant, often predominant, amounts of β-carotene and lutein, although chlorophyll masks the yellow color.[1,29,30] Understanding β-carotene signal in leaves is important as an indicator of plant health. The TLC-Raman methodology introduced here could be applied to correlate plant health status with the concentration of β-carotene or other specific carotenoids found in the leaves. As a provitamin A carotenoid, β-carotene is also vital to human health,[1] and our TLC-Raman protocol could also be used to assess the β-carotene content of plants to obtain nutritional information.

Experimental

Materials

TLC silica gel 60 F254 plates, Whatman® grade 1 filter paper, ethyl acetate, petroleum ether, and chlorophyll a from spinach were purchased from Millipore. Octane and chloroform were purchased from Sigma. Acetone was purchased from Sigma and Fisher. Cyclohexane was purchased from Thermo. Ethanol was purchased from Decon Labs. *Trans*-β-carotene was obtained from Aldrich. Lutein was purchased from Cayman Chemical. Magnesium carbonate basic pentahydrate ($MgCO_3$) was purchased from Strem Chemicals. All purchased chemicals were used without further purification.

Tomato plant growth conditions

Three tomato plants (*Solanum lycopersicum* 'Better Boy') were grown outdoors on a patio with partial shade in Columbus, OH during the summer. Young tomato plants, roughly 6 in. tall, were obtained from Strader's Garden Center, Columbus, Ohio, and planted in pots containing potting soil and Jobe's tomato fertilizer spikes. Plants were watered regularly.

Handheld Raman spectroscopy of tomato leaves and pigment standards

Handheld Raman spectra were acquired from the leaves of all three tomato plants during the fruiting stage after 4 months of growth. These measurements were performed outdoors in the evening at the location of plant growth. A Metrohm MiraDS handheld device with a 785 nm laser and intelligent Universal Attachment was used to collect data. Each spectrum was acquired for 2 s with 37 mW of power delivered to the sample in orbital raster scanning mode. Three leaves from each of the three tomato plants were randomly chosen for sampling. While keeping the leaves intact on the plant, a Raman spectrum was recorded from three different spots on each of the three leaves. Reference Raman spectra of solutions of β-carotene and lutein in nonpolar solvents (octane and chloroform, respectively) on gold-coated glass slides were also collected using the handheld device for comparison to signals from leaves.

Tomato leaf extractions

Samples of leaf tissue from the three tomato plants were collected in a plastic bag and frozen at −20 °C. To extract plant material, approximately 200 mg of tissue was transferred to an Eppendorf tube and frozen in liquid nitrogen. The tube was shaken with two 4 mm metal beads on a homogenizer at 15 Hz for 40 s for a total of 2 cycles. The resulting pulverized material was soaked in 1 mL of acetone with a small scoop of $MgCO_3$ for 15 min at 4 °C. The tube was centrifuged at 15 000rcf for 15 min at 4 °C, then the supernatant was filtered through a 0.2 μm nylon disc syringe filter into a glass test tube. The extract was dried completely under a nitrogen stream while protected from light for 50 min. The dried extract was stored at 4 °C in the dark until resuspension in 200 μL of acetone for TLC experiments.

Tomato leaf extract spiking with β-carotene

A β-carotene stock solution was prepared in acetone at a concentration of 0.150 μg μL^{-1}. Three samples of tomato leaf extract were spiked with different amounts of β-carotene. First, a 40 μL sample of tomato leaf extract was spiked with 40 μL of

the stock β-carotene solution (6 μg of β-carotene), giving a spike of 0.0750 μg μL^{-1}. A second 40 μL sample of tomato leaf extract was mixed with 20 μL of acetone and 20 μL of the stock β-carotene solution (3 μg of β-carotene), achieving a spike of 0.0375 μg μL^{-1}. A third 40 μL sample of tomato leaf extract was diluted with 40 μL of acetone (0 μg of β-carotene), creating an unspiked sample.

Thin layer chromatography (TLC)

All thin layer chromatography (TLC) experiments were performed using a rectangular developing tank (17.5 cm × 16.0 cm × 8.2 cm) and reverse phase silica plates (5 cm × 10 cm). The mobile phase, consisting of petroleum ether : cyclohexane : ethyl acetate : acetone : ethanol (60 : 16 : 10 : 10 : 6 v/v), was selected based on an optimized protocol for leaf pigment separation by Hynstova *et al.*[31] Mobile phase and Whatman® filter paper were added to the developing tank, which was covered with a glass plate to equilibrate. TLC plates were spotted with samples using either 2 μL drops or 5 μL drops from a micropipette. Sample spots were placed 1 cm from the bottom of the plate, and each plate was designed with 2 lanes equally spaced from one another to ensure sufficient spacing with no overlap between spots. Each spot was allowed to dry before adding the next.

Calibration curves were created for β-carotene quantification by TLC-Raman and TLC-UV-Vis. A 0.067 μg μL^{-1} stock solution of β-carotene in acetone was prepared. Different numbers of drops of stock solution were spotted onto the TLC plate to achieve various masses of β-carotene with a consistent spot size. More specifically, Table 1 shows the number of 2 and 5 μL drops used to prepare the plates with several known masses of β-carotene. A UV-Vis calibration curve was created using 5 μL drops, and two different TLC-Raman curves were created for comparison-one with 2 μL drops and one with 5 μL drops.

For acquisition of data from unspiked and β-carotene-spiked extracts, TLC plates were spotted with 2 μL drops of sample for Raman analysis, and separate TLC plates were spotted with 5 μL drops for UV-Vis analysis. A consistent volume of each sample totaling 20 μL was spotted onto the plate for both analysis methods to simplify comparisons of resulting quantities. In other words, either 10–2 μL drops or 4–5 μL drops were used for each extract sample spot.

All plates spotted with calibration and test samples were developed in the TLC chamber with the previously described mobile phase until the solvent front reached approximately

Table 1 Amounts of β-carotene stock solution used to create TLC-Raman and TLC-UV-Vis calibration curves

Mass of β-carotene (μg)	Number of 2 μL drops	Number of 5 μL drops
0	0	0
0.67	5	2
1.3	10	4
2.7	20	8
4.0	30	12
5.3	40	16

1 cm from the top of the plate. Plates were removed from the TLC chamber, and the solvent front was quickly marked using a soft graphite pencil. The farthest traveling edge of the β-carotene spot was also marked, and the R_f values for each plate were recorded. Photos of each plate were taken immediately after the solvent dried.

Handheld Raman spectroscopy of spots on TLC plates

Handheld Raman spectra were collected from TLC plates using a power of 23 mW in orbital raster scanning mode with an acquisition time of 10 s each. Three replicate spectra were recorded from each β-carotene spot on the TLC plates. Measurements were made immediately after removing plates from the chamber to avoid sample degradation. Spectral collection from other TLC spots was attempted, but intense fluorescence was observed. No silica background was observed from the plate.

UV-Vis spectroscopy of spots from TLC plates

For UV-Vis analysis, the TLC spots corresponding to β-carotene were quickly cut out from the TLC plates immediately after removing them from the chamber. The resulting plate pieces were submerged in 500 μL of acetone in Eppendorf tubes. The silica was thoroughly scraped off from the aluminum backing into the acetone. The tubes were vortexed, shaken at 800 rpm for 4 min, and vortexed again to ensure solvation of all β-carotene present in the spot. The tubes were then centrifuged at 3000 rcf for 1 min to pellet the silica. The supernatant was transferred into a quartz microcuvette, carefully avoiding the silica. UV-Vis spectra were collected from the supernatant samples using a Cary 4000 UV-Vis spectrophotometer in double beam mode from 200.0 to 800.0 nm. Three replicate spectra were recorded from each sample. Before the measurements, the instrument was baselined with acetone.

Data processing and analysis

Spectral analysis, including preprocessing and plotting, was performed in MATLAB (R2019b, The Mathworks Inc.). Raman spectra of leaves were baseline corrected using a "rolling-circle filter" in MATLAB.[32] Peak fitting was performed using "peakfit" in MATLAB.[33] Peak fitting results were exported to Excel (Version 16.78, Microsoft) for further processing, such as calculating averages, creating scatter plots, and performing linear regression and error calculations.

Results and discussion

Collection of handheld Raman spectra from the tomato leaves (Fig. 1A) reveals a signature with peaks at 623, 642, 707, 748, 1005, 1157, 1187, 1213, 1289, 1321, 1386, 1435, 1527, 1551, and 1606 cm^{-1} (Fig. 1B). Our findings agree with previous reports of Raman spectra from plant leaves.[8–10,12] These studies identify carotenoids as a major source of the Raman signal of leaves, although specifying which specific carotenoids is laborious and often not explored further by Raman spectroscopy methods.
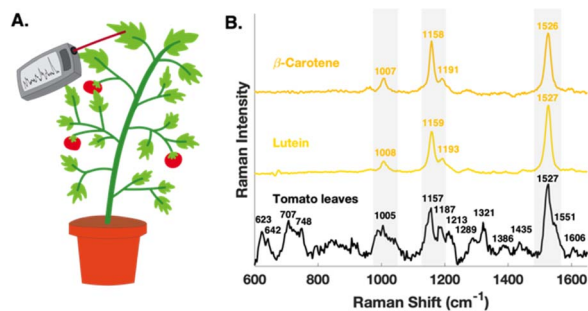
Fig. 1 Handheld Raman signal acquired from tomato leaves. (A) Scheme illustrating the acquisition of Raman spectra from the leaves of a tomato plant using a handheld device. (B) Average baselined, handheld Raman spectra from leaves of tomato plants and from β-carotene and lutein in solution for comparison. Signals demonstrate good agreement, as indicated by peaks in highlighted regions.
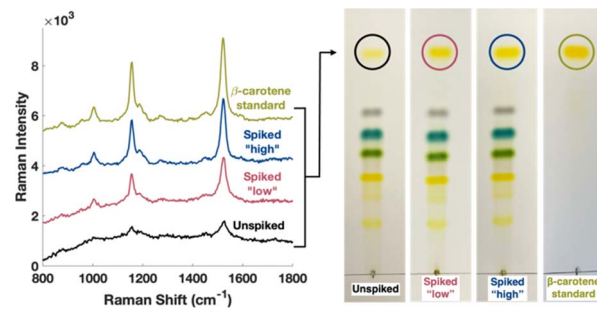

Fig. 2 Average Raman spectra and images obtained from TLC plates spotted with samples of tomato leaf extract, β-carotene-spiked tomato leaf extract, and β-carotene standard (2.7 μg). Spectra are offset for clarity. Drops of 2 μL were used to spot all samples. R_f values for all plates are 0.9.

In the context of this work, reference Raman spectra of β-carotene and lutein, common carotenoids which are found in high concentrations in plant leaves,[29] were collected using the handheld instrument. The quality and purity of the carotenoid standards were confirmed by electrospray ionization liquid chromatography-mass spectrometry (ESI LC-MS) as shown in Fig. S1.† β-carotene in octane, a highly nonpolar solvent, displays Raman bands at 1007, 1158, 1191, and 1526 cm^{-1} (Fig. 1B). The signals from β-carotene dissolved in other, more polar solvents show slightly shifted C=C stretching frequencies (Fig. S2†). Lutein poses solubility challenges in highly nonpolar solvents like octane, but it does not display significant solvatochromatic shifts (Fig. S2†). Dissolved in moderately nonpolar chloroform, lutein exhibits Raman signal at 1008, 1159, 1193, and 1527 cm^{-1} (Fig. 1B). The comparison of Raman signals in Fig. 1B shows strong agreement and suggests that β-carotene and lutein in nonpolar environments, such as plastidic membranes, may contribute significantly to the leaf spectra. However, from these *in vivo* leaf spectra alone it cannot be determined with certainty which specific carotenoids are present, or in what quantities they are present, in the tomato leaves. The Raman spectra are also comprised of signals which arise from other leaf components besides carotenoids.

For further investigation of the carotenoid content of the leaves, pigments were isolated by performing extractions of tomato leaf material. Of the carotenoids with detectable Raman signal, β-carotene was chosen as the focus for further study. Samples of extract were spiked with varying amounts of β-carotene to create unspiked (+0.00 μg/20 μL), spiked "low" (+0.75 μg/20 μL), and spiked "high" (+1.50 μg/20 μL) versions of the sample. Thin layer chromatography (TLC) was utilized to separate 20 μL of the various extracted pigments into their pure components on silica plates. As shown in Fig. 2, β-carotene travels farthest on the plate (top yellow-orange spot), with significant separation from the other pigments, which include pheophytins (gray), chlorophylls (green), and xanthophylls (yellow), listed from top to bottom.[31]

Handheld Raman spectra of the β-carotene spots obtained directly from the TLC plates are shown in Fig. 2. The positions

of the Raman bands observed from the unspiked extract, the spiked extracts, and the β-carotene standard all coincide at 1005, 1157, 1187, and 1522 cm^{-1}. The intensity and saturation of the color of the β-carotene spots on the plates visibly increase with increasing amount of β-carotene spike. Additionally, the R_f values of each measured spot are consistent, which further validates the identity of the spots as β-carotene.

To quantify the β-carotene in the extracts using the TLC-Raman signals, a calibration curve was constructed based on the peak area of the C=C stretch at 1522 cm^{-1} for various amounts of β-carotene spotted onto TLC plates (Fig. 3). This curve demonstrates a detection limit of 0.03 μg and a quantification limit of 0.10 μg of β-carotene as calculated using the method described in the ESI.† Images of TLC plates used to build the curve can be referenced in Fig. S3.†

Effectively designing a quantitative TLC-Raman protocol requires several important considerations. For plate spotting, using a consistent sample volume with a variable drop number ensures that the sample distributes in a uniform and controlled area, regardless of analyte mass loaded onto the plate. Optimizing the sample spot size, or determining drop volume, to suit instrumentation is also key. In our case, the spot size obtained from 2 μL drops ensures that the entirety of the raster scanning laser fits within the analyte spot without leaving
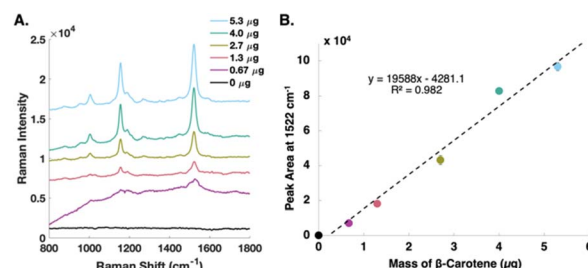

Fig. 3 Raman spectroscopy-based calibration curve for β-carotene on TLC plate. (A) Average Raman spectra from different quantities of β-carotene spotted onto TLC plate using 2 μL drops. Spectra are offset for clarity. (B) Plot of average peak area at 1522 cm^{-1} as a function of β-carotene mass loaded onto TLC plate. Standard deviations are included as error bars.

a significant portion of the sample unprobed. Notably, for our TLC-Raman experiments with β-carotene, using a larger drop size of 5 μL shows lower sensitivity and decreased linear fit as compared to 2 μL drops (Fig. S4†). The detection limit (0.06 μg) and quantification limit (0.21 μg) are also higher with the larger drops. Using a larger volume, the sample spreads out more on the plate, giving a smaller mass per area and effectively reducing the intensity of Raman signal obtained from the sample. Thus, the smaller drop size is ideal for TLC-Raman quantification.

The TLC-Raman calibration curve (Fig. 3B) was used to ascertain the amount of β-carotene present in the spiked and unspiked leaf extract samples. Reported as average ± standard error in x in Table 2, the unspiked solution contains 0.53 ± 0.23 μg, the spiked "low" solution contains 1.24 ± 0.21 μg, and the spiked "high" solution contains 1.98 ± 0.20 μg. In terms of the amount of spike detected, the calculated values are 0.71 ± 0.21 μg and 1.45 ± 0.20 μg, as compared to the actual values of 0.75 μg and 1.50 μg. These experimental values demonstrate percent errors of 5.3% and 3.3%. The excellent agreement between the calculated values and the actual values supports the viability of TLC-Raman for β-carotene quantification in leaf extract samples.

The quantities of β-carotene determined by TLC-Raman were validated by UV-Vis characterization. Concentrations of total carotenoids in leaf extracts can be determined directly by UV-Vis.[34] However, absorbance bands from multiple pigments overlap in the 400–500 nm region where β-carotene absorbs light, so separation techniques are useful to achieve UV-Vis signal uniquely from β-carotene. UV-Vis signals of β-carotene from unspiked and spiked leaf extracts spotted onto TLC plates are shown in Fig. 4A.

A TLC-UV-Vis calibration curve for β-carotene was created using the absorbance at 452 nm from different masses of β-carotene standard developed on TLC plates (Fig. 4B and C). Images of these calibration plates are provided in Fig. S3.† This UV-Vis curve shows a detection limit of 0.02 μg and a quantification limit of 0.05 μg of β-carotene, which is slightly lower than that of the TLC-Raman curve. The UV-Vis method shows good validation of the β-carotene quantities determined by the Raman method. A summary of the quantification results obtained from each of the leaf extract samples by Raman and UV-Vis is reported in Table 2.

Additionally, a standard addition curve was created using the UV-Vis data from the extract samples (Fig. S5†). This method
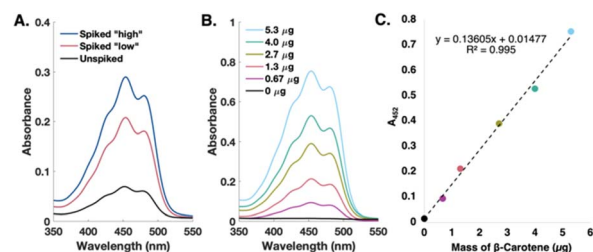

Fig. 4   TLC–UV-Vis quantification for β-carotene from TLC plate. (A) UV-Vis spectra of leaf extract and β-carotene-spiked leaf extracts, showing increased absorbance at 452 nm after each instance of spiking. (B) UV-Vis spectra of different quantities of β-carotene from TLC plate dissolved in acetone. (C) Plot of absorbance at 452 nm, where Beer−Lambert law is used to determine the amount of β-carotene present.

gives a value of 0.54 ± 0.14 μg of β-carotene present in the original, unspiked extract sample, which is reported with standard deviation in concentration (S_x) from the standard addition curve. This quantity also matches the quantity calculated using the TLC-Raman method.

The Raman spectra of the other leaf pigment TLC spots besides β-carotene show significant fluorescence (Fig. S6†), making TLC-Raman detection of these molecules challenging. Nonetheless, this approach can also be used to quantify other carotenoids from leaves, such as lutein from spinach. The TLC-Raman calibration curve for lutein (Fig. S7†) gives an LOD of 0.03 μg and reveals the presence of 0.70 ± 0.20 μg of lutein in 20 μL of spinach extract (Fig. S8†). The Raman signal from lutein standard on the TLC plate (Fig. S7†) does not display fluorescence. This finding suggests that the background observed from the leaf-derived lutein spot is attributable to additional molecules which co-elute with lutein on the plate. The UV-Vis signal from the TLC spot of lutein from spinach extract (Fig. S9†) indicates the presence of molecules which absorb around 330 nm, likely phenolic compounds such as flavonoids.[35] To effectively utilize TLC-Raman for quantification of the higher polarity pigments with lower R_f values, an additional separation step, extraction method, or the TLC mobile phase composition could be optimized to remove interfering molecules from the leaf extract solution. Finally, our TLC-Raman method proves useful for carotenoid quantification but has limitations in detecting leaf pigments which are inherently fluorescent at the chosen excitation wavelength, such as chlorophyll (Fig. S10†).

Table 2   Summary of β-carotene in tomato leaf extracts quantified by TLC–Raman and validated by TLC–UV-Vis. Measured values exhibit good agreement with actual amount of β-carotene used to spike each sample. Values are reported as average ± standard error in x of measurements

Sample	Detected mass (μg) by Raman	Detected mass (μg) by UV-Vis	Calculated spike (μg) by Raman	Calculated spike (μg) by UV-Vis	Actual spike (μg)
Unspiked	0.53 ± 0.23	0.40 ± 0.11	—	—	—
Spiked "low"	1.24 ± 0.21	1.42 ± 0.10	0.71 ± 0.21	1.01 ± 0.10[a]	0.75
Spiked "high"	1.98 ± 0.20	2.01 ± 0.10	1.45 ± 0.20	1.61 ± 0.10	1.50

[a] Value could be slightly elevated due to sample evaporation during plate preparation.

Conclusions

In conclusion, we have developed a novel quantitative TLC-Raman assay for carotenoids with high sensitivity and low error. These measurements are performed using an affordable separation method with handheld Raman equipment in less than half an hour, whereas previously established methods require considerably more time and resources. The ability to obtain Raman spectra of carotenoids, such as β-carotene, directly from the TLC plate is crucial to simultaneously confirming the identity and the quantity of the specific carotenoid. This technique could be utilized to better elucidate the relationships between carotenoid concentrations in leaves and degree of plant health. For instance, the link between β-carotene content and health factors such as plant stress, disease states, or fertilization status could be further studied. Chlorophyll quantification by Raman at 785 nm remains difficult due to fluorescence, but an alternative excitation wavelength could be implemented to mitigate this issue. Moreover, TLC-Raman could be utilized to reveal the pigmentation properties of plant tissues besides green leaves, and additional TLC-Raman methods could be optimized to track other pigments, such as lycopene or anthocyanins. The technique could also be expanded to study different classes of pigmented materials altogether. Overall, the TLC-Raman methods developed here will help scientists better understand the exact molecular origin of the pigment signals obtained from plant leaves and the conditions under which these species are found in increased or decreased amounts. Ultimately, this knowledge could have exciting applications in ecology, agriculture, metabolic engineering, and many other fields.

Author contributions

Conceptualization, T. D. P., L. R. D., F. C. S., A. E. B., and Z. D. S; methodology, T. D. P., L. R. D., F. C. S., and J. J. B.; investigation, T. D. P., L. R. D., and F. C. S.; formal analysis, T. D. P., L. R. D., and F. C. S.; visualization, T. D. P., L. R. D., and F. C. S.; writing, reviewing and editing, T. D. P., L. R. D., F. C. S., J. J. B., A. E. B., and Z. D. S.; funding acquisition, A. E. B. and Z. D. S.; resources, J. J. B. and Z. D. S.; supervision, Z. D. S.

Conflicts of interest

There are no conflicts to declare.

Acknowledgements

References

1 T. Sun, S. Rao, X. Zhou and L. Li, *Mol. Hortic.*, 2022, **2**, 3.

2 T. Maoka, *J. Nat. Med.*, 2020, **74**, 1–16.

3 M. Havaux, *Plant J.*, 2014, **79**, 597–606.

4 X. Hou, J. Rivers, P. León, R. P. McQuinn and B. J. Pogson, *Trends Plant Sci.*, 2016, **21**, 792–803.

5 J. C. Moreno, J. Mi, Y. Alagoz and S. Al-Babili, *Plant J.*, 2021, **105**, 351–375.

6 J. Mi, J. G. Vallarino, I. Petřík, O. Novák, S. M. Correa, M. Chodasiewicz, M. Havaux, M. Rodriguez-Concepcion, S. Al-Babili, A. R. Fernie, A. Skirycz and J. C. Moreno, *Metab. Eng.*, 2022, **70**, 166–180.

7 M. Shumskaya and E. T. Wurtzel, *Plant Sci.*, 2013, **208**, 58–63.

8 S. Gupta, C. H. Huang, G. P. Singh, B. S. Park, N.-H. Chua and R. J. Ram, *Sci. Rep.*, 2020, **10**, 20206.

9 N. Altangerel, G. O. Ariunbold, C. Gorman, M. H. Alkahtani, E. J. Borrego, D. Bohlmeyer, P. Hemmer, M. V. Kolomiets, J. S. Yuan and M. O. Scully, *Proc. Natl. Acad. Sci. U.S.A.*, 2017, **114**, 3393–3396.

10 S. Yeturu, P. Vargas Jentzsch, V. Ciobotă, R. Guerrero, P. Garrido and L. A. Ramos, *Anal. Methods*, 2016, **8**, 3450–3457.

11 V. Egging, J. Nguyen and D. Kurouski, *Anal. Chem.*, 2018, **90**, 8616–8621.

12 S. Higgins, S. Biswas, N. K. Goff, E. M. Septiningsih and D. Kurouski, *Front. Plant Sci.*, 2022, **13**, 754735.

13 N. Gong, F. Yao, J. Wang, W. Fang, C. Sun and Z. Men, *Opt. Express*, 2020, **28**, 33068.

14 M. Macernis, J. Sulskus, S. Malickaja, B. Robert and L. Valkunas, *J. Phys. Chem. A*, 2014, **118**, 1817–1825.

15 N. Tschirner, M. Schenderlein, K. Brose, E. Schlodder, M. A. Mroginski, C. Thomsen and P. Hildebrandt, *Phys. Chem. Chem. Phys.*, 2009, **11**, 11471.

16 P. Gupta, Y. Sreelakshmi and R. Sharma, *Plant Methods*, 2015, **11**, 5.

17 V. V. De Rosso and A. Z. Mercadante, *J. Agric. Food Chem.*, 2007, **55**, 5062–5072.

18 A. Zeb and F. Ullah, *Front. Chem.*, 2017, **5**, 29.

19 L. M. Londoño-Giraldo, M. Bueno, E. Corpas-Iguarán, G. Taborda-Ocampo and A. Cifuentes, *Horticulturae*, 2021, **7**, 272.

20 T. Dou, L. Sanchez, S. Irigoyen, N. Goff, P. Niraula, K. Mandadi and D. Kurouski, *Front. Plant Sci.*, 2021, **12**, 680991.

21 S. Higgins, V. Serada, B. Herron, K. R. Gadhave and D. Kurouski, *Front. Plant Sci.*, 2022, **13**, 1035522.

22 A. P. Holman, N. K. Goff, I. D. Juárez, S. Higgins, A. Rodriguez, M. Bagavathiannan, D. Kurouski and N. Subramanian, *RSC Adv.*, 2024, **14**, 1833–1837.

23 K. István, G. Keresztury and A. Szép, *Spectrochim. Acta, Part A*, 2003, **59**, 1709–1723.

24 C. Petty and N. Cahoon, *Spectrochim. Acta, Part A*, 1993, **49**, 645–655.

25 F. Pozzi, N. Shibayama, M. Leona and J. R. Lombardi, *J. Raman Spectrosc.*, 2013, **44**, 102–107.

26 M. Zhang, Q. Yu, J. Guo, B. Wu and X. Kong, *Biosensors*, 2022, **12**, 937.

27 X. Sha, S. Han, G. Fang, N. Li, D. Lin and W. Hasi, *Food Control*, 2022, **138**, 109040.

28 Z.-M. Zhang, J.-F. Liu, R. Liu, J.-F. Sun and G.-H. Wei, *Anal. Chem.*, 2014, **86**, 7286–7292.

29 M. Raju, S. Varakumar, R. Lakshminarayana, T. Krishnakantha and V. Baskaran, *Food Chem.*, 2007, **101**, 1598–1605.

30 M. Li, G. Y. Jang, S. H. Lee, M. Y. Kim, S. G. Hwang, H. M. Sin, H. S. Kim, J. Lee and H. S. Jeong, *Food Sci. Biotechnol.*, 2017, **26**, 97–103.

31 V. Hynstova, D. Sterbova, B. Klejdus, J. Hedbavny, D. Huska and V. Adam, *J. Pharm. Biomed. Anal.*, 2018, **148**, 108–118.

32 I. K. Mikhailyuk and A. P. Razzhivin, *Instrum. Exp. Tech.*, 2003, **46**, 765–769.

33 T. O'Haver, *peakfit.m, Version 9.0.0.0*, 2018, **https://www.mathworks.com/matlabcentral/fileexchange/23611-peakfit-m2023**.

34 K. J. Scott, *Curr. Protoc.*, 2001, F2.2.1–F2.2.10.

35 I. Spiridon, R. Bodirlau and C.-A. Teaca, *Open Life Sci.*, 2011, **6**, 388–396.